PHYSICAL REVIEW B **90**, 020101(R) (2014)

Ab initio design of charge-mismatched ferroelectric superlattices

Claudio Cazorla[1,*] and Massimiliano Stengel[1,2]
[1]*Institut de Ciència de Materials de Barcelona (ICMAB-CSIC), 08193 Bellaterra, Spain*
[2]*ICREA - Institució Catalana de Recerca i Estudis Avançats, 08010 Barcelona, Spain*
(Received 14 February 2014; revised manuscript received 25 June 2014; published 21 July 2014)

We present a systematic approach to modeling the electrical and structural properties of charge-mismatched superlattices from first principles. Our strategy is based on bulk calculations of the parent compounds, which we perform as a function of in-plane strain and out-of-plane electric displacement field. The resulting two-dimensional phase diagrams allow us to accurately predict, without performing further calculations, the behavior of a layered heterostructure where the aforementioned building blocks are electrostatically and elastically coupled, with an arbitrary choice of the interface charge (originated from the polar discontinuity) and volume ratio. By using the $[PbTiO_3]_m/[BiFeO_3]_n$ system as test case, we demonstrate that interface polarity has a dramatic impact on the ferroelectric behavior of the superlattice, leading to the stabilization of otherwise inaccessible bulk phases.

DOI: 10.1103/PhysRevB.90.020101 PACS number(s): 71.15.−m, 77.22.Ej

When layers of perovskite oxides are epitaxially stacked to form a periodically repeated heterostructure, new intriguing functionalities can emerge in the resulting superlattice [1,2]. These are further tunable via applied electric fields and thermodynamic conditions, and thus attractive for nanoelectronics and energy applications. An excellent example is the $[PbTiO_3]_m/[SrTiO_3]_n$ system, where the polarization, tetragonality, piezoelectric response, and ferroelectric transition temperature strongly change with the volume ratio of the parent compounds [3–5]. Such a remarkable tunability is usually rationalized in terms of epitaxial strains [6], electrostatic coupling [see Fig. 1(a)] [7,8], and local interface effects [9,10].

While perovskite titanates with the $ATiO_3$ formula (A = Sr, Pb, Ba, or Ca) have traditionally been the most popular choice as the basic building blocks, a much wider range of materials (e.g., $BiFeO_3$) is currently receiving increasing attention by the community. The motivation for such an interest is clear: a superlattice configuration provides the unique opportunity of enhancing materials properties via "strain engineering," and a multifunctional compound such as $BiFeO_3$ appears to be a natural candidate in this context [11,12]. Also, a superlattice geometry can alleviate the leakage issues observed in pure $BiFeO_3$ films [13,14].

Combining a III–III perovskite such as $BiFeO_3$ (or I–V, such as $KNbO_3$) with a II–IV titanate appears, however, problematic from the conceptual point of view. In fact, the charge-family mismatch inevitably leads to polar (and hence electrostatically unstable) interfaces between layers [15]. This is not necessarily a drawback, though: recent research has demonstrated that polar interfaces can be, rather than a nuisance to be avoided, a rich playground to be exploited for exploring exciting new phenomena. The prototypical example is the $LaAlO_3/SrTiO_3$ system, where a metallic two-dimensional electron gas appears at the heterojunction to avoid a "polar catastrophe" [16,17]. Remarkably, first-principles calculations have shown that interfaces in oxide superlattices can remain insulating provided that the layers are thin enough, and produce rather dramatic effects on the respective polarization of the individual components [15,18]. This means that, in a superlattice, polar discontinuities need not be compensated by electronic or ionic reconstructions; they can, instead, be used as an additional, powerful materials-design tool to control the behavior of the polar degrees of freedom therein. Such a control may be realized, for instance, by altering the stoichiometry at the interfaces [see Fig. 1(b)]. To fully explore the potential that this additional degree of freedom (the interface built-in polarity) provides, and guide the experimental search for the most promising materials combinations, one clearly needs to establish a general theoretical framework where the "compositional charge" [15] is adequately taken into account.

In this Rapid Communication, we present a general first-principles approach to predict the behavior of charge-mismatched perovskite oxide superlattices based exclusively on the properties of their individual bulk constituents. Our formalism combines the constrained-D strategies of Wu *et al.* [19], which are key to decomposing the total energy of the system into the contributions of the individual layers, with the rigorous description of the interface polarity proposed in Ref. [20]. As a result, we are able to exactly describe the electrostatic coupling and mechanical boundary conditions, enabling a clear separation between genuine interface and bulk effects. Crucially, the present method allows one to quantify, in a straightforward way, the impact that interface polarity has on the equilibrium (and metastable) phases of the superlattice. As a proof of concept we apply our formalism to the study of $[PbTiO_3]_m/[BiFeO_3]_n$ (PTO/BFO) heterostructures. We find that (i) our *bulk* model accurately matches earlier first-principles predictions obtained for ultrashort-period superlattices (i.e., $m = n = 3$) by using explicit *supercell* simulations [21], and (ii) by assuming interface terminations with different nominal charge, we obtain a radical change in the overall ferroelectric properties of the superlattice, which demonstrates the crucial role played by the polar mismatch.

We start by expressing the total energy of a monodomain two-color superlattice (i.e., composed of species A and B) as

$$U_{\rm tot}(D,\lambda,a) = \lambda \cdot U_{\rm A}(D,a) + (1-\lambda)\cdot U_{\rm B}(D,a). \quad (1)$$

Here $U_{\rm A}$ and $U_{\rm B}$ are the internal energies of the individual constituents, D is the electric displacement along the out-of-plane

*ccazorla@icmab.es

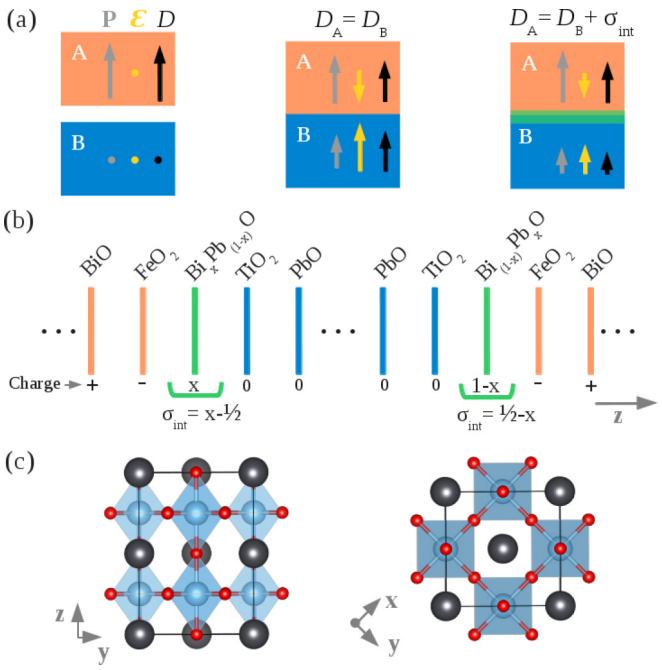

FIG. 1. (Color online) (a) Description of the electrostatic coupling in a ferroelectric (orange)/paraelectric (blue) bilayer; P, $\mathcal{E}$, D, and $\sigma_{\rm int}$ are explained in the text. (b) Intermixed AO-type interfaces in a $[BiFeO_3]_m/[PbTiO_3]_n$ superlattice and the resulting interface charge densities. (c) Illustration of the 20-atom simulation cell used in our calculations; red, blue, and black spheres represent O, B, and A atoms in ABO_3 perovskites.

stacking direction (i.e., $D \equiv \mathcal{E} + 4\pi P$ where $\mathcal{E}$ is the electric field and P is the *effective* polarization, relative to the centrosymmetric reference configuration), λ is the relative volume ratio of material A [i.e., $\lambda \equiv m/(n+m)$ where m and n are the thicknesses of layers A and B, respectively], and a is the in-plane lattice parameter (we assume heterostructures that are coherently strained to the substrate). Note that short-range interface effects have been neglected. (While it is certainly possible to incorporate the latter in the model, e.g., along the guidelines described in Ref. [19], these would have been an unnecessary complication in the context of the present study as we discuss further below.) By construction, Eq. (1) implicitly enforces the continuity of D along the out-of-plane stacking direction (which we label as z henceforth), which is appropriate for superlattices where the interfaces are nominally uncharged [1,2].

In the presence of a polar mismatch, one has a net "external" interface charge of compositional origin [15], $\sigma_{\rm int}$ [see Fig. 1(a)], which is localized at the interlayer junctions. In such a case, Eq. (1) needs to be revised as follows:

$$U_{\rm tot}(D,\sigma_{\rm int},\lambda,a) = \lambda \cdot U_{\rm A}(D,a) + (1-\lambda)\cdot U_{\rm B}(D-\sigma_{\rm int},a); \quad (2)$$

i.e., the $U_{\rm B}$ curve is shifted in D space to account for the jump in D produced by $\sigma_{\rm int}$. (Recall the macroscopic Maxwell equation, $\nabla\cdot\mathbf{D} = \rho_{\rm ext}$, where $\rho_{\rm ext}$, the "external" charge, encompasses all contributions of neither dielectric nor ferroelectric origin [15,20].) Once the functions $U_{\rm A}$ and $U_{\rm B}$ are computed and stored (e.g., by using the methodology of Ref. [22]), one can predict the ground state of a hypothetical A/B superlattice by simply finding the global minimum of $U_{\rm tot}$ with respect to D at fixed values of $\sigma_{\rm int}$, λ, and a. The advantage of this procedure is that, for a given choice of A and B, the aforementioned four-dimensional parameter space can be explored very efficiently, as no further *ab initio* calculations are needed. Note that the applicability of Eq. (2) is by no means restricted to first-principles models. One can trivially apply the same strategy to macroscopic theory (i.e., by replacing $U_{\rm A}$ and $U_{\rm B}$ with the appropriate Landau-like free energy functionals).

It is useful, before going any further, to specify the physical origin of $\sigma_{\rm int}$ in the context of this work. Consider, for example, a periodic $BiFeO_3/PbTiO_3$ superlattice, which we assume (i) to be stoichiometric (and therefore charge-neutral) as a whole, (ii) to have an ideal AO-BO_2-AO-BO_2 stacking along the (001) direction, and (iii) to form (say) AO-type interfaces [see Fig. 1(b)]. (The same arguments can be equally well applied to the case of BO_2-type interfaces.) Depending on the growth conditions, one can have a certain degree of intermixing in the boundary AO layers, which will adopt an intermediate composition $Bi_x\,Pb_{(1-x)}O$ [or $Bi_{(1-x)}\,Pb_xO$]. As a pure BiO layer is formally charged $+1$ and PbO is neutral, the net formal charge of such interface layer is x [or $1-x$] (expressed in units of e/S with S being the surface of the corresponding 5-atom perovskite cell). Now, the total "compositional" interface charge $\sigma_{\rm int}$ must also include (see Refs. [23,24]) the contribution of the *built-in* (non-switchable) polarity of BFO (the individual BiO and FeO_2 layers carry a formal charge of $+1$ and -1, respectively). We thus obtain $\sigma_{\rm int} = \pm(x-\frac{1}{2})$, where the choice of plus or minus depends on the arbitrary assignment of $BiFeO_3$ and $PbTiO_3$ as the A or B component in Eq. (2) [see Fig. 1(b)]. In the following we shall illustrate the crucial role played by $\sigma_{\rm int}$ (and hence, by the interface stoichiometry) on the ferroelectric properties of a BFO/PTO superlattice, by combining Eq. (2) with the bulk $U_{\rm BFO}(D,a)$ and $U_{\rm PTO}(D,a)$ curves that we calculate from first principles.

Our calculations are performed with the "in-house" LAUTREC code within the local spin density approximation to density functional theory. (We additionally apply a Hubbard $U = 3.8$ eV to Fe ions [25,26].) We use the 20-atom simulation cell depicted in Fig. 1(c) for both BFO and PTO, which allows us to describe the ferroelectric and antiferrodistortive (AFD) modes of interest (i.e., in-phase AFD_{zi} and out-of-phase AFD_{zo} and AFD_{xy}; see Ref. [10]). Atomic and cell relaxations are performed by constraining the out-of-plane component of D [22] and the in-plane lattice constant a to a given value. [Calculations are repeated in order to span the physically relevant two-dimensional (D,a) parameter space.]

We start by illustrating the results obtained at fixed strain, $a = 3.81$ Å (see Fig. 2), by assuming $\sigma_{\rm int} = 0$, which corresponds to fully intermixed junctions ($x = 0.5$), and we vary the BFO volume ratio, λ. At the extreme values of λ, the results are consistent with the expectations: the equilibrium configuration of BFO (i.e., the minimum of $U_{\rm tot}$ with $\lambda = 1$) at this value of a is the well-known R-type Cc-I phase [27], derived from the bulk ground state via the application of epitaxial compression; PTO ($\lambda = 0$), on the other hand, is in a tetragonal $P4mm$ phase with the polarization vector oriented out of plane. Intermediate values of λ yield a linear combination of the two single-component $U(D)$ curves, where

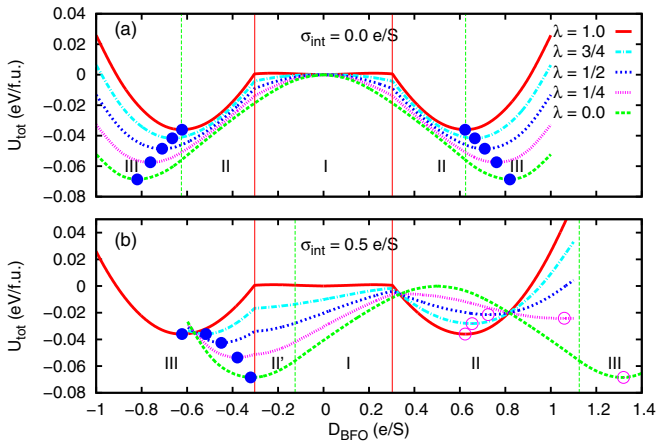

FIG. 2. (Color online) Energy of PTO/BFO superlattices with $a = 3.81$ Å expressed as a function of D, for selected values of λ and $\sigma_{\rm int}$ (where $D_{\rm PTO} = D_{\rm BFO} - \sigma_{\rm int}$). Equilibrium and metastable superlattice states are represented with solid and empty dots. Red (green) vertical lines indicate phase transitions occurring in bulk BFO (PTO) under different D conditions. (a) and (b) represent the cases of neutral and polar interfaces, respectively.

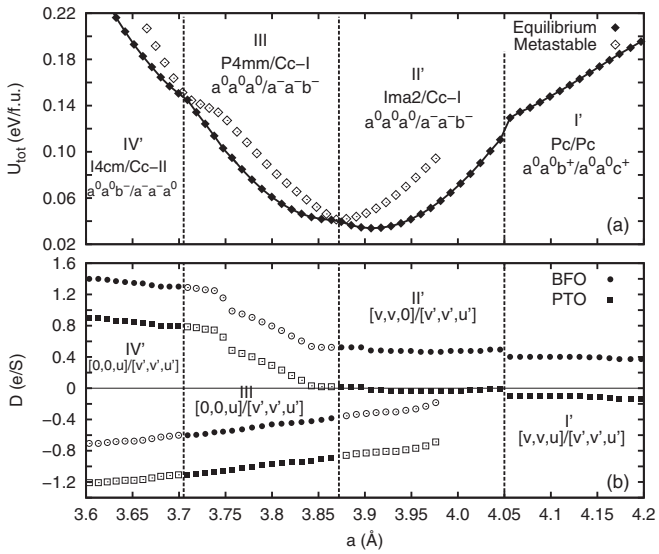

FIG. 3. Total energy (a) and out-of-plane electric displacement D (b) of the equilibrium (solid symbols) and metastable (empty symbols) states of PTO/BFO superlattices with $\lambda = \frac{1}{2}$ and $\sigma_{\rm int} = 0.5$, expressed as a function of the in-plane lattice parameter. Regions in which PTO and BFO exist in different phases are delimited with vertical dashed lines; the corresponding space groups and AFD distortion patterns in Glazer's notation are shown in (a), and the components of the ferroelectric polarization in (b).

the spontaneous P_z at equilibrium gradually moves from the pure PTO to the pure BFO value.

Unfortunately, the possible equilibrium states that can be attained by solely varying λ (at this value of a and $\sigma_{\rm int}$) lie far from any physically "interesting" region of the phase diagram. For example, note the kink at $|D| \sim 0.3$ C/m^2 in the pure BFO case, which corresponds to a first-order transition to an orthorhombic $Pna2_1$ phase (a close relative of the higher-symmetry $Pnma$ phase, occurring at $D = 0$). A huge piezoelectric and dielectric response is expected in BFO in the vicinity of the transition [28], raising the question of whether one could approach this region by playing with $\sigma_{\rm int}$, in addition to λ.

The answer is yes: when oxide superlattices with $\sigma_{\rm int} = 0.5$ are considered [corresponding to "ideal" $(BiO)^+/TiO_2$ and $(FeO_2)^-/PbO$ interfaces], the stable minimum of the system favors a smaller spontaneous polarization in the BFO layers, approaching the aforementioned (Cc−I $\rightarrow Pna2_1$) phase boundary in the limit of small λ. Interestingly, the $U_{\rm tot}(D)$ curve becomes asymmetric (the interfacial charge breaks inversion symmetry), and a secondary, metastable minimum appears. Overall, the resulting phase diagram turns out to be much richer, with new combinations of phases emerging (e.g., in region II′, where BFO exists in the orthorhombic $Pna2_1$ phase and PTO in the tetragonal $P4mm$ phase) and highly nontrivial changes in the electrical properties occurring as a function of λ.

In order to further illustrate the power of our approach, we shall now fix the volume ratio to $\lambda = 0.5$ (corresponding to alternating BFO and PTO layers of equal thickness) and vary the in-plane lattice parameter in the range $3.6 \leqslant a \leqslant 4.2$ Å. We shall first consider the case of charged interfaces with $\sigma_{\rm int} = 0.5$, as this choice allows for a direct comparison with the results of Yang *et al.* (obtained via standard supercell simulations) [21]. In Fig. 3 we show the energy and spontaneous electric displacement of the equilibrium and metastable states as a function of a. Four regions can be identified in the diagrams depending on the phases adopted by BFO and PTO at each value of the in-plane strain. (Their crystal space groups, AFD pattern, and in-plane/out-of-plane ferroelectric polarization, respectively P_{xy} and P_z, are specified in compact form in the figure.) In region I′ both PTO and BFO adopt a monoclinic Pc phase characterized by large in-phase AFD_z distortions and nonzero P_{xy} and P_z. Such a monoclinic Pc phase is closely related to the orthorhombic $Pmc2_1$ structure which has been recently predicted in PTO and BFO at large tensile strains [26]. In region II′ PTO adopts an orthorhombic $Ima2$ phase, characterized by vanishing AFD distortions and a large in-plane **P** (we neglect the small out-of-plane P_z), while BFO is in its well-known Cc-I state. In region III, BFO remains Cc-I, while PTO adopts a $P4mm$ phase, both with *opposite* out-of-plane polarization with respect to region II′. These structures switch back to a positively oriented P_z in region IV′, respectively transforming into a monoclinic Cc-II and a tetragonal $I4cm$ phase. The $I4cm$ phase is characterized by antiphase AFD_z distorsions and an out-of-plane **P**, while the Cc-II corresponds to the "supertetragonal" T-type phase of BFO [29]. Note that, as observed already while discussing Fig. 2, the net interface charge leads to an asymmetric double-well potential, and consequently to an energy difference [typically of ∼20 meV/f.u. or less; see Fig. 3(a)] between the two oppositely polarized states. (Only one minimum survives at large tensile strains, where the superlattice is no longer ferroelectric.) At the phase boundaries such energy difference vanishes; the obvious kinks in the $U_{\rm tot}$ curve shown in Fig. 3(a) indicate that the transitions (at $a = 3.71$, 3.87, and 4.05 Å) are all of first-order type.

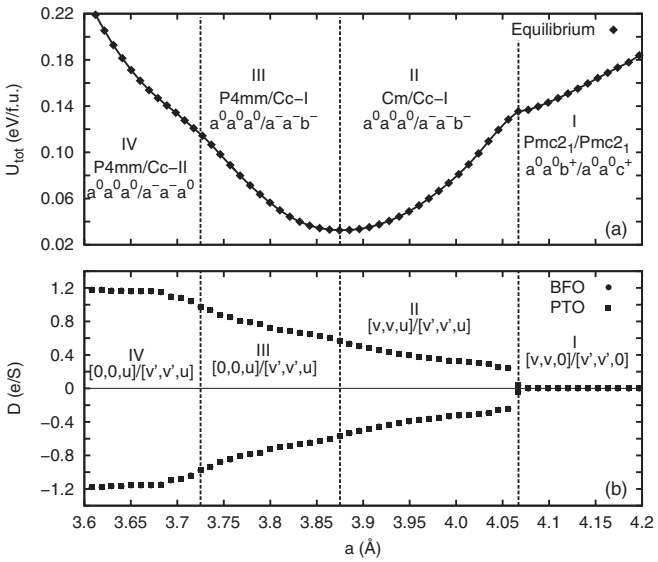

FIG. 4. Same as in Fig. 3, but considering neutral interfaces. The out-of-plane polarization is the same in PTO and BFO layers.

The above results are in remarkable agreement with those of Yang *et al.* [21]. The only apparent discrepancy concerns the ordering of the stable/metastable states in region III, which anyway involves a very subtle energy difference (and is therefore sensitive to short-range interface effects, not considered here). Obtaining such an accurate description of superlattices where the individual layers are as thin as three perovskite units [21] provides a stringent benchmark for our method, and validates it as a reliable modeling tool. From the physical point of view this comparison suggest that, even in the ultrathin limit, PTO/BFO superlattices can be well understood in terms of macroscopic bulk effects; i.e., short-range interface-specific phenomena appear to play a relatively minor role. The same conclusion could apply reasonably well also to a wide number of perovskite systems, although this should be explicitly checked in each particular case [30].

Having gained confidence in our method, we can use it to predict the behavior of a hypothetical superlattice with $\sigma_{\rm int} = 0$, corresponding to a centrosymmetric reference structure with fully intermixed $Pb_{0.5}Bi_{0.5}O$ interface layers (see Fig. 4). Note the symmetry of the two opposite polarization states, and the common value of the spontaneous electric displacement adopted by BFO and PTO. The resulting phase diagram consists, again, of four regions, with a first-order and two second-order phase transitions occurring at $a = 4.07$, 3.88, and 3.73 Å, respectively [see Fig. 4(a)]. In three of these regions, the individual layers display structures which are different from those obtained in the $\sigma_{\rm int} = 0.5$ case: in region I both PTO and BFO stabilize in an orthorhombic $Pmc2_1$ phase [26], characterized by a vanishing P_z; in region II PTO adopts a monoclinic Cm phase with the polarization roughly oriented along (111) ($P_z \neq P_{xy} \neq 0$) and no AFD, while BFO stabilizes in the already discussed Cc-I phase; finally, in region IV, PTO is tetragonal $P4mm$ and BFO is monoclinic Cc-II. These findings quantitatively demonstrate that the interface charge mismatch can have a tremendous impact on the physical properties of oxide superlattices. Our simple and general method allows one to accurately model and quantify these effects, and most importantly to rationalize them in terms of intuitive physical concepts.

In summary, we have discussed a general theoretical framework to predict the behavior of charge-mismatched superlattices. We have showed that the effect of the interface stoichiometry, which we describe via the "compositional" interface charge $\sigma_{\rm int}$, is quite dramatic, and needs to be properly accounted for in the models. More generally, we argue that $\sigma_{\rm int}$ can be regarded, in addition to λ and a, as a further degree of freedom in designing oxide heterostructures with tailored functionalities, opening exciting new avenues for future research.

This work was supported by MICINN-Spain (Grants No. MAT2010-18113 and No. CSD2007-00041) and the CSIC JAE-DOC program (C.C.). We thankfully acknowledge the computer resources, technical expertise, and assistance provided by RES and CESGA.

[1] P. Ghosez and J. Junquera, J. Comput. Theor. Nanosci. **5**, 2071 (2008).
[2] C. Lichtensteiger *et al.*, in *Oxide Ultrathin Films: Science and Technology*, edited by G. Pacchioni and S. Valeri (Wiley-VCH, Germany, 2011), Chap. 12, p. 265.
[3] M. Dawber, C. Lichtensteiger, M. Cantoni, M. Veithen, P. Ghosez, K. Johnston, K. M. Rabe, and J. M. Triscone, Phys. Rev. Lett. **95**, 177601 (2005).
[4] M. Dawber *et al.*, Adv. Mater. **19**, 4153 (2007).
[5] J. Sinsheimer, S. J. Callori, B. Bein, Y. Benkara, J. Daley, J. Coraor, D. Su, P. W. Stephens, and M. Dawber, Phys. Rev. Lett. **109**, 167601 (2012).
[6] M. Dawber, K. M. Rabe, and J. F. Scott, Rev. Mod. Phys. **77**, 1083 (2005).
[7] P. Zubko *et al.*, Nano Lett. **12**, 2846 (2012).
[8] C. W. Swartz and X. Wu, Phys. Rev. B **85**, 054102 (2012).
[9] P. Aguado-Puente, P. García-Fernández, and J. Junquera, Phys. Rev. Lett. **107**, 217601 (2011).
[10] E. Bousquet, M. Dawber, N. Stucki, C. Lichtensteiger, P. Hermet, S. Gariglio, J.-M. Triscone, and P. Ghosez, Nature (London) **452**, 732 (2008).
[11] J. C. Wojdeł and J. Íñiguez, Phys. Rev. Lett. **103**, 267205 (2009).
[12] J. C. Wojdeł and J. Íñiguez, Phys. Rev. Lett. **105**, 037208 (2010).
[13] R. Ranjith, B. Kundys, and W. Prellier, Appl. Phys. Lett. **91**, 222904 (2007).
[14] R. Ranjith *et al.*, Appl. Phys. Lett. **92**, 232905 (2008).
[15] E. D. Murray and D. Vanderbilt, Phys. Rev. B **79**, 100102 (2009).
[16] N. Nakagawa, H. Y. Hwang, and D. A. Muller, Nat. Mater. **5**, 204 (2006).
[17] A. Ohtomo and H. Y. Hwang, Nature (London) **427**, 423 (2004).

[18] N. C. Bristowe, E. Artacho, and P. B. Littlewood, Phys. Rev. B **80**, 045425 (2009).
[19] X. Wu, M. Stengel, K. M. Rabe, and D. Vanderbilt, Phys. Rev. Lett. **101**, 087601 (2008).
[20] M. Stengel and D. Vanderbilt, Phys. Rev. B **80**, 241103(R) (2009).
[21] Y. Yang, M. Stengel, W. Ren, X. H. Yan, and L. Bellaiche, Phys. Rev. B **86**, 144114 (2012).
[22] M. Stengel, N. A. Spaldin, and D. Vanderbilt, Nat. Phys. **5**, 304 (2009).
[23] D. Vanderbilt and R. D. King-Smith, Phys. Rev. B **48**, 4442 (1993).
[24] M. Stengel, Phys. Rev. B **84**, 205432 (2011).
[25] I. A. Kornev, S. Lisenkov, R. Haumont, B. Dkhil, and L. Bellaiche, Phys. Rev. Lett. **99**, 227602 (2007).
[26] Y. Yang, W. Ren, M. Stengel, X. H. Yan, and L. Bellaiche, Phys. Rev. Lett. **109**, 057602 (2012).
[27] A. J. Hatt, N. A. Spaldin, and C. Ederer, Phys. Rev. B **81**, 054109 (2010).
[28] C. Cazorla and M. Stengel (unpublished).
[29] R. J. Zeches *et al.*, Science **326**, 977 (2009).
[30] S. M. Nakhmanson, K. M. Rabe, and D. Vanderbilt, Appl. Phys. Lett. **87**, 102906 (2005).